Journal of Environmental Management 281 (2021) 111852

Contents lists available at ScienceDirect

Journal of Environmental Management

journal homepage: http://www.elsevier.com/locate/jenvman

Immobilization and retention of caffeine in soil amended with *Ulva reticulata* biochar

S. Keerthanan [a], Chaminda Gunawardane [b], Thiruchenduran Somasundaram [c], Tharuka Jayampathi [d,e], Chamila Jayasinghe [f], Meththika Vithanage [a,*]

[a] Ecosphere Resilience Research Center, Faculty of Applied Sciences, University of Sri Jayewardenepura, Nugegoda, 10250, Sri Lanka
[b] National Institute of Post Harvest Management, Jayanthi Mawatha, Anuradhapura, Sri Lanka
[c] School of Life and Environmental Sciences, Faculty of Science, Engineering and Built Environment, Deakin University, Warrnambool, Victoria, 3280, Australia
[d] School of Agriculture, Food and Wine, University of Adelaide, Waite Campus, Urrbrae, SA, Australia
[e] School of Biosciences, University of Nottingham, Sutton Bonington Campus, Loughborough, Leicestershire, UK
[f] Department of Food Science and Technology, Faculty of Livestock, Fisheries and Nutrition, Wayamba University of Sri Lanka, Makandura, Gonawila, Sri Lanka

ARTICLE INFO

Keywords:
Soil amendment
Caffeine
Emerging contaminants
Biochar
Pharmaceuticals and personal care products

ABSTRACT

The goal of the present study was to evaluate the immobilization and retention of caffeine (CFN) in soil and the influence of biochar for the CFN transport in agricultural soil. The biochar was produced from the *Ulva reticulata* seaweed biomass (ULBC) under the slow-pyrolysis with a heating rate of 7 °C/min at 500 °C and characterized using XRD and FTIR. The CFN retention and transport abilities in loamy sand and ULBC amended (2.5%) soil were evaluated under various pH values range of 3–10 and at various CFN concentrations using batch and column experiments. The surface orientation of ULBC was portrayed as the randomized distribution of hetero and homogeneous nature. The highest retention capacity (40 μg/g) was obtained at pH 4.0. Soil amendment with ULBC shows a higher retention affinity towards CFN, of up to 150 μg/g than soil, with minimal pH dependence. The maximum CFN adsorption capacities of soil and amended soils were 420 and 820 μg/g, respectively, based on the Langmuir model. Batch experiments suggested the adsorption of CFN by the biochar amended loamy soil is governed by the electrostatic attraction. The column experiment data demonstrated a high transport potential of CFN in the loamy sand; however, a strong cumulative reduction of transport (58%) was observed with the application of ULBC into the loamy sand. Thus, the addition of seaweed biochar as an amendment in soils with biosolids and wastewater irrigation may reduce the mobilization of CFN to the aquatic system and possibly reduce plant uptake.

1. Introduction

Pharmaceutical and Personal Care Products (PPCPs) are considered critical emerging substances in the environment globally. PPCPs are reported in the wastewater, surface water, and groundwater at a wide range, ranging from ng/L to mg/L, and soil at μg/kg (Keerthanan et al., 2020). Commonly, the persistence of PPCPs in the environment is via the commercial and domestic pathways, including landfill leachates of municipal solid waste, the effluent of wastewater treatment plants and hospitals, fertilization of farmland with PPCPs contaminated biosolids, irrigation of wastewater to the agricultural lands, waste from PPCPs manufacturing companies, discharging of expired products, and household use of cosmetics items (Balakrishna et al., 2017; Madikizela et al., 2018; Tasho and Cho, 2016). Recently, the ubiquitous detection of PPCPs in the environment was fast-track in both developed and developing countries due to the ineffectiveness of the wastewater treatment plants and haphazard disposal, respectively. For example, in China (Liu et al., 2020), Sri Lanka (Guruge et al., 2019), France (Miossec et al., 2019), Canada (Kleywegt et al., 2019), and India (Balakrishna et al., 2017). The occurrence of PPCPs in the environment can cause a deleterious effect on the environment and terrestrial and aquatic organisms, including humans (Li et al., 2015, 2020a, 2020b).

Caffeine (CFN) is one such compound that is being used simultaneously as pharmaceutical as well as a personal care product. CFN is considered an emerging pollutant due to its high detection in the environment (Keerthanan et al., 2020; Luo et al., 2014; Zhang et al., 2014).

* Corresponding author.
E-mail address: meththika@sjp.ac.lk (M. Vithanage).

https://doi.org/10.1016/j.jenvman.2020.111852
Received 12 September 2020; Received in revised form 7 December 2020; Accepted 13 December 2020
Available online 1 January 2021

For instance, the occurrence of CFN in the effluent water of the embalming process in Canada was found at 14,200 μg/L (Kleywegt et al., 2019) while, CFN was detected in effluent water of a research city in Ny-Ålesund, Svalbard at 230 μg/L (Choi et al., 2020). Further, the presence of CFN in lagoon-water, which received high anthropogenic stress, was detected as 20 μg/L in Saudi Arabia (Picó et al., 2020) and 96 μg/L in an influent of the wastewater treatment plant in Greece (Kosma et al., 2014). The high detection of CFN in water media can be due to the frequent and excessive use of it, high water solubility (21.6 g/L), low octanol-water partition coefficient (log $K_{ow} = 0.16$), and high half-life in the environment (3.5–100 days) (Álvarez-Torrellas et al., 2016). Although CFN is a natural product, it can cause deleterious human health issues when consumed over 200 mg/day. Once CFN is ingested by a human, 1–10% of it can be excreted by the urine. For instance, about 4 μM of CFN was reported in the human urine after the consumption of coffee by the authors of Martínez-López et al. (2014).

The mobilization of CFN from the aquatic environment to soil was taken place mainly via wastewater irrigation of the agricultural lands in Beijing, China (Ma et al., 2018). Soil concentration of CFN was detected as high as 2.9 μg/kg in vadose zone soils irrigated with wastewater, groundwater, and river water (Ma et al., 2018). Further, the maximum CFN concentration in a surface soil sample near a community housing scheme was 25.44 μg/kg (Picó et al., 2020). Once CFN reached the agricultural soil, it can be taken up by crops (Keerthanan et al., 2020) and enter human diets (Dodgen et al., 2014). Thus, the high CFN concentrations can cause a negative impact on the environment, humans, and non-target organisms. For example, the allelopathy impact of CFN on the growth of lettuce seedling was reported in Pham et al. (2019). The range of 10–100 mg/L CFN in water can develop an anxiety behavior in hatchling of Japanese rice fish and affect the early development stage in zebrafish (Korekar et al., 2019). Chronic consumption of CFN can cause serious human health risks such as behavioral changes, pregnancy deficiency, and intercellular effects (Jain et al., 2019; Qian et al., 2019; Volkow et al., 2015). Significantly, CFN increases the risk of calcium oxalate precipitation in kidneys in modest amounts (Massey and Sutton, 2004). Therefore, the remediation of CFN from the environmental matrices through a cost-effective approach is an essential and a timely need.

Biochar is a carbonized biomass at a specific temperature in an oxygen-less atmosphere (Zhao et al., 2018). It is used in the remediation of organic (Jayawardhana et al., 2019; Li et al., 2018) and inorganic (Li et al., 2020a, 2020b) pollutants from the wastewater, limitation of the passage of environmental fate and transport (Vithanage et al., 2014), and supporting the improvement of soil fertility viaincreased nutrient retention and reduced N_2O emission from agricultural soils (Ahmad et al., 2014; Manyà, 2012; Roberts et al., 2015). Hence, the application of biochar to the agricultural land may support in fulfilling four sustainable development goals of no poverty (SDG 1), zero hunger (SDG 2), good health and well-being (SDG 3), and clean water and sanitation (SDG 6). In any case, studies are lacking on remediation of caffeine-rich soil with biochar amendment, though CFN is found in agricultural soils.

Recently, seaweed biomass received attention as a feedstock for biochar due to the enormous annual production, which exceeds over 19 million tons as a food source (Roberts et al., 2015). The conversion of seaweed to biochar reduces the coastal seaweed problem. It is reported that the biochar derived from the seaweed biomass has a lower carbon content than those derived from woody biomass (Roberts and de Nys, 2016). However, the seaweed biochar has higher mineral content such as N, K, Mg, Ca, P, Mo, and Zn than that of the other biochars, which inducedplant growth, especially in lower fertility agricultural soil (Roberts and de Nys, 2016). The seaweed biochar has been successfully applied to the remediation of remazol from the wastewater (Gokulan et al., 2019). However, the soil adsorption of CFN, correctly using seaweed biochar has not been reported in previous studies to the authors' knowledge. Therefore, the objectives of the present study were (1) the utilization of *Ulva reticulata* seaweed for biochar production at 500 °C temperature as a soil-biochar amendment, (2) to assess the mobilization and retention of CFN by soil and soil-seaweed biochar amendment at variable pH and different initial concentrations of CFN in wastewater.

2. Material and methods

2.1. Chemicals

CFN (98.5%) was obtained from Sisco Research Laboratories Pvt. Ltd. (India). NaOH and HCl were obtained from Sigma Aldrich (USA) for pH changes. FTIR grade KBr (>99%) used to make pellet was also purchased from Sigma Aldrich. The HPLC grade acetonitrile, glacial acetic acid, and phosphoric acid were purchased from Sigma Aldrich (Germany). Ultra-pure water (conductivity, 0.05 μS/cm) was obtained from Smart2pure 6 UV, Thermo scientific, Germany.

2.2. Soil collection

The soil sample was collected at a depth of 0–5 cm from Colombo, Sri Lanka, where no wastewater discharge was noted. The soil collection method was adopted from Swami (2017). In brief, a v-shaped cut was made in the soil up to about 5 cm depth. Thick slices of soil were collected into a plastic bag and transferred to the laboratory. The collected soil was air-dried for 3 days and sieved through a 2 mm mesh. Finally, the sieved soil was stored in a polythene bag at room temperature until the begining of the experiments.

2.3. Biochar production

The biomass of Ulva reticulata was collected from the seashore at Beruwala, Sri Lanka (6°28′41.3″N 79°58′58.1″E). The biomass was rinsed many times in distilled water to remove excess salt. It was then dried in open air, crushed and ground, and passed through a 500 μm sieve. The pyrolysis conditions were maintained based on the previous publication of Ahmad et al. (2013) and Rajapaksha et al. (2015). In brief, the biomass was pyrolyzed at 500 °C with a heating rate of 7 °C/min under the limited oxygen atmosphere in a muffle furnace (P330, Nabertherm, Germany). A mid-temperature of 500 °C has been chosen since the seaweeds are light in stable carbon and high in minerals (Roberts et al., 2015). Once the pyrolysis reaches the peak temperature, the process was continued for 2 h: Hereafter, the obtained biochar was ground and sieved through 250 μm mesh and mentioned as ULBC.

2.4. Characterization of soil, biochar, and soil-biochar amendment

The pH and electrical conductivity (EC) in a suspension of soil/ULBC/ULBC amended soil and ultra-pure water at 1:10 (w/v) ratio were measured using a pH meter (AD1030, Adwa, Romania) equipped with a pH electrode (AD1131B, Adwa, Romania) and a conductivity meter (EUTECH Con 450, Thermo scientific) respectively. Cation exchange capacity (CEC) was estimated using a method adopted in Gunarathne et al. (2020). In brief, the soil sample was saturated with CH_3COONH_4 (1 M) solution at pH 7.0. Afterward, the solution was centrifuged at 2500 rpm for 15 min and filtered using a syringe filter (Labfil-PTFE hydrophobic, C0000300, China). The filtrate was analyzed for Na^+, K^+, Mg^{2+}, and Ca^{2+} by using Micro-Plasma Atomic Emission Spectroscopy (MP-AES) (4210, Agilent, USA).

The proximate analysis of ULBC was experimented based on the method described by Ahmad et al. (2013). Briefly, the moisture content of ULBC was calculated by estimating the weight-loss after 24 h of oven-drying at 105 °C. The mobile matter of ULBC was examined by a method of heating the biochar at 450 °C for 1 h in a closed crucible. The ash content of ULBC was determined by heating the biochar at 750 °C for 1 h in an opened crucible. The resident matter was determined by subtracting the total percentage of moisture content, ash content, and

mobile matter. The morphological investigation on the ULBC surface was carried out using a field emission scanning electron microscope (SEM, SU6600 FESEM; Hitachi, Ltd., Tokyo, Japan). KBr pellet Fourier-transform infrared spectroscopy (FTIR; Thermo Scientific, Nicolet iS10 spectrometer, USA) with bandwidth ranging from 500 to 4000/cm was used to record the FTIR spectra. The atmospheric interference, noise reduction, background correction was performed by OMNIC software (Version 6, Thermo Nicolet, USA). The Powder X-ray Diffraction (PXRD) diffractogram of soil, ULBC, and amendment soil were obtained from a Rigaku, Ultima IV (Japan) diffractometer. The diffractometer was operated at 40 mA and 40 kV using radiation of Cu Kα. The diffractogram was recorded from 3° to 85° (2θ scale) at a record rate of 2°/min. The zero-point charge (pHzpc) of soil and soil amendment was determined by a pH drift method adopted from Tran et al. (2017). In brief, the initial pH (pHi) of NaCl solution (25 mL) as a background electrolyte was adjusted between 2 and 12 using NaOH (1 M) and HCl (1 M) under the nitrogen purging environment. To the resulting solutions, 75 mg of adsorbent added and were shaken at 150 rpm in a water-bath shaker (Gemmyco YCW-012S, Taiwan). After 48 h of shaking, the final pH (pHf) was noted. Finally, the pHzpc was determined from the plot of pHi-pHf against pHi.

2.5. High-performance liquid chromatography analysis

An Ultra-High-Performance Liquid Chromatography (UHPLC) system (Ultimate 3000, Thermo Scientific, USA) equipped with an autosampler and UV–Vis detector was used to analyze CFN. A mixture of HPLC grade acetonitrile and 0.1%phosphoric acid at 20:80 v/v ratio served as a mobile phase (Lopez-Sanchez et al., 2018; Ornaf and Dong, 2005). The mobile phase was pumped through the column (Altima C18 10 μm, 250 × 4.6 mm) at 1 mL/min of flow rate, and CFN was detected by UV–Vis detector at 270 nm. The injection volume of the sample was 20 μL, and CFN standards ranging from 1 to 10 mg/L were used in the calibration and the concentrations of solutions were diluted between the calibration range. The limit of detection and limit of quantification of this method were 0.001 and 0.004 mg/L, respectively. Five level calibration series was prepared and which showed a higher linearity R^2 = 0.99997. The residual concentration of the calibration solution was varied between −0.03 and 0.02. Quality control samples were prepared at a high concentration of 10 mg/L CFN solution simultaneously with the same experimental conditions. The mean concentration of CFN in the quality control solution was 10.19 ± 0.07, n = 3.

2.6. pH edge experiment

The effect of pH on the retention of CFN in soil with and without amendment of ULBC was conducted at pH ranging from 3 to 10 at room temperature (25 °C). The pH of the experimental solution was adjusted using 0.1 M HCl and NaOH (Atugoda et al., 2020). The pH effect was investigated using 50 g/L of soil and soil with 2.5% of ULBC suspension in 10 mg/L of CFN solution based on the obtained quality performance in maintaining the soil properties (Bandara et al., 2017). The resulting mixtures were placed on an orbital shaker (Rotabit, Selecta) for 12 h at 500 rpm to attain equilibrium, measured the pHs, centrifuged at 2000 rpm and filtered using a 0.45 μm syringe filter (Labfil-PTFE hydrophobic, C0000300, China). Finally, the equilibrium strength of CFN in the solution was determined using a UHPLC.

2.7. Batch isotherm experiment

The effect of CFN strength on soil adsorption with and without the ULBC amendment was investigated with different initial concentrations of CFN ranging between 10 and 500 mg/L at pH 4.0 (optimum pH) and 25 °C, shaken for 12 h and processed for analysis.

2.8. Soil column and leaching experiment

The soil columns (height: 10 cm and diameter: 2.7 cm) were made in 50 mL centrifuge tubes. The soil with and without the ULBC amendment was wet-filled into the columns. The porosity and pore volume of columns were 40 ± 2% and 20 ± 1 mL, respectively. Initially, the columns were saturated and preconditioned by feeding about 2 pore volumes (40 mL) of ultra-pure water in steady gravitational flow. A total of 8 pore volumes of 10 mg/L of CFN solution was fed into the columns. Subsequently, a 15 pore volume of ultra-pure water was flowed through the column in atmospheric conditions to estimate the leaching of CFN in the soil. The resultant leachate solutions were filtered and analyzed.

The contaminated soil from both soil and ULBC amended soil columns were further investigated to determine the CFN leachability in soil by toxicity characteristic leaching procedure (TCLP) adopted from Ahmadi et al. (2016) and Vithanage et al. (2017). In brief, 1 g of soil was placed in a centrifuge tube (50 mL) containing acetic acid solution (20 mL) with a pH of 2.89. The resultant mixtures were kept on an orbital shaker for 18 h at 250 rpm. The suspensions were filtered and the concentration of CFN was determined.

2.9. Data analysis and modeling

The CFN adsorption capacity and distribution coefficient (*Kd*) of the soil and the soil-ULBC amendment was calculated using equations (1) and (2). The isotherm model was achieved using a non-linear isotherm model of Freundlich, Langmuir, and Temkin regression using equations (3), (4) and (6), respectively. The data modeling was performed by using the Origin 2018 software package.

$$Q_e = (C_i - C_e)^* v / M \tag{1}$$

$$Q_e = Kd^* C_e \tag{2}$$

$$Q_e = k_F C_e^n \tag{3}$$

$$Q_e = (Q_{max} k_L C_e)/(1 + k_L C_e) \tag{4}$$

$$R_L = 1/(1 + k_L C_i) \tag{5}$$

$$Q_e = \frac{RT}{b} \ln(A_T C_e) \tag{6}$$

$$B = RT/b \tag{7}$$

where, Q_e (mg/g) is CFN adsorption capacity, C_i and C_e (mg/L) are initial and equilibrium CFN concentrations respectively, v (L) is solution volume, M (g) amount of soil and soil-ULBC amendment, k_F ((mg/g)/(mg/L)^n) is Freundlich constant related to adsorption capacity, n is adsorption intensity, Q_{max} (mg/g) is maximum adsorption capacity, k_L(L/mg) is Langmuir constant, R_L is a unitless separation factor, R (J/mol·K) is gas constant, T (K) is absolute temperature, b is Temkin constant, and A_T (L/mg) is Temkin equilibrium binding constant, B is the heat of adsorption (J/mol).

The soil and amendment column experiment results were modeled with two commonly used models of Yoon-Nelson and Thomas models to understand the kinetic behavior of CFN through the soil and ULBC amended soil packed columns. The mathematical expression of linear Yoon-Nelson and Thomas models provided in equations (8) and (9) respectively were used for this purpose (Singh et al., 2017).

$$\ln \frac{C}{C_o - C} = K_{YN} t - \tau K_{YN} \tag{8}$$

$$ln\left(\frac{C_o}{C} - 1\right) = \frac{k_{TH} q_{TH} M}{Q} - k_{TH} C_o t \tag{9}$$

$$q_{YN} = \frac{\tau C_o Q}{1000M} \quad (10)$$

where, C_o and C are referred to as influent and effluent concentrations of CFN, respectively. The K_{YN}, τ, and t are termed as a Yoon-Nelson rate constant (1/min), time is taken to adsorb 50% of CFN by soil or amended soil (min), and time taken to collect pore volumes of solution through the columns (min). The k_{TH}, q_{TH}, M and Q are known as Thomas rate constant (mL/mg·min), Thomas uptake capacity (mg/g), the mass of soil packed in columns, and flow rate of CFN solution through the columns (mL/min).

The adsorption capacity related to Yoon-Nelson model was estimated as a function of M, C_o, τ, and Q using equation (10) (Singh et al., 2017).

3. Results and discussion

3.1. Characteristics of soil, ULBC, and ULBC-soil amendment

The physical and chemical parameters of soil, ULBC, and ULBC amended soil are provided in Table 1. The tested soil was slightly acidic, with a pH value of 6.39. Generally, the undissociated form of organic acids in the soil pH below the pKa value of respective acid was existed (Xu et al., 2009), resulting in weak adsorption between soil and organic adsorbates (Clofibric acid). The pH of ULBC was 10.26, which indicates the discharging of acidic functional groups and alkali metals during the pyrolysis (Keerthanan et al., 2020b). The application of ULBC to the soil increased the soil pH to 7.86. A similar pattern of change in the EC was observed (Table 1). The soil texture was identified as loamy sand with sand (85%), silt (5%), and clay (10%). The CEC range of 1–5, 5–10, 5–15, 15–30, and >30 cmol/kg respectively, estimate the texture of sand, fine sandy loam, loam, clay loam, and clay. Further, the CEC value of 3–15, 15–40, and 80–100 cmol/kg elaborate the contained clay components of kaolinite, illite, and montmorillonite (Sonon et al., 2017). The CEC of experimental soil was estimated as 3.84 cmol/kg, indicating that soil texture was sandy with kaolinite clay.

The ash content of ULBC was estimated as higher (38.36%), which indicates that the *Ulva* biochar is rich in micro and macronutrients such as Na, K, Ca, Mg, N, P, Zn, and Mo (Roberts and de Nys, 2016). The SEM images at different magnifications are shown in Fig. 1. A randomized morphology appeared on the surface of ULBC. The heterogeneous and homogeneous nature can be seen on the ULBC surface with randomly distributed different-sized porous structures during the pyrolysis at 500 °C. The variation of the surface morphology can provide more affinity sites to the CFN adsorption (Keerthanan et al., 2020a).

The FTIR spectrum of soil, pristine ULBC, CFN-loaded soil, CFN-loaded ULBC amended soil, and CFN are shown in Fig. 2(a)–(e) respectively. In the spectrum of soil shown in Fig. 2(a), a sharp stretching peak at 3695/cm ascribes the presence of a free –OH group of clay minerals in the soil matrix (Xing et al., 2019). Two stretching sharp peaks at 3619 and 3523/cm could indicate the existence –NH_2 group belongs to primary amine and/or amide (Pavia et al., 2001). A characteristic stretching pulse of –OH at 3431/cm describes the occurrence of alcohols and/or carboxylic groups in the experimental soil (Álvarez et al., 2015). Furthermore, the stretching vibrations at 2923 and 2854, 1633, and bending peak at 1245/cm belongs to the functional groups of aliphatic –CH_2– and –CH_3, C═O of amide and/or carboxylic and/or C═C, and C–N (Ben-Ali et al., 2017; Jiang and Hu, 2019; Pavia et al., 2001) respectively, due to the presence of humic material in the soil. The stretching pulses at 1108 and 1033/cm can be originated from the functional groups of Si–O–Si and C–O (Shenzhen, 2015). A sharp pulse at 1005 and 913/cm can be ascribed to the stretching of Si–O and Al–OH in silicate and kaolinite presence in soil (Xing et al., 2019). Frequencies assigned to the –NH_2 out of the plane and iron oxides were observed at 794 and 689/cm, respectively, in the soil (Xing et al., 2019; Xu et al., 2020). Hence, the FTIR spectrum of soil suggested the experimental soil may contain organic matter, silicate, kaolinite, and iron oxide.

In the FTIR spectrum of ULBC shown in Fig. 2 (b), a broad oscillation at 3398/cm can be assigned to –OH belonging to phenol or carboxylic functional group (Álvarez et al., 2015). The stretching pulse generated at 2920 and 2851/cm can be attributed to the aliphatic –CH_2– and –CH_3 groups present in derived ULBC (Pavia et al., 2001). Moreover, the vibration that appeared at 1636/cm may be described as the presence of C═O and/or C═C functional groups on the surface of ULBC (Keerthanan et al., 2020a). The peak at 1150/cm originated from the stretching frequency for Si–O, which was previously observed in the seaweed and freshwater algae-derived biochar by Lu et al. (2017) and Michalak et al. (2019).

The CFN adsorbed soil and amended soil's FTIR spectra, as shown in Fig. 2 (c) and (d). No new peaks were observed in the CFN adsorbed to the soil. However, the shifting and broadening of existing peaks can be observed in the CFN adsorbed to the soil. The characteristic stretching peak of –CH_3 was appeared at 2917/cm in the CFN adsorbed to the soil, and this peak was initially been at 2923/cm in the soil. The C═O stretching and C–H bending peaks were found at 1630 and 1383/cm in the CFN adsorbed soil and which were initially found at 1633 and 1386/cm, respectively, in the soil. These changes in the positions of the peaks may be indicated the incorporation of CFN with soil (Keerthanan et al., 2020b). Similarly, the peak of –CH_3 stretching shifted and increased in intensity at 2917/cm in the CFN adsorbed amended soil, and it was initially at 2923/cm in soil and 2920/cm in ULBC. Moreover, the C═O stretching, C–H bending, and C–N stretching oscillations at 1630, 1383, and 1274/cm respectively in the CFN loaded amended soil, and these pulses were formerly observed at 1633, 1386, and 1245/cm in the soil and 1636 and 1386/cm in ULBC. Hu et al. (2019) observed the FTIR characteristic peaks shifting in agricultural soils after the loading of sulfamethoxazole and sulfadiazine. These changes in the peaks manifested the successful incorporation of CFN molecules in the amended soil.

The PXRD diffractogram of ULBC is shown in Fig. 3 (a). Sharp peaks observed in ULBC at 2θ = 15°–35° indicated the presence of different minerals such as silicate, calcite, sodium chloride, magnesium oxide (Kim et al., 2011). The 2θ = 31.5°, 2θ = 29.3°, and 2θ = 25.5° refer to the peak of sodium chloride (Zhang et al., 2020), calcite (Kim et al., 2011), and SiO_2/quartz (Liu et al., 2012) respectively. Moreover, the presence of quartz in the ULBC was confirmed by the FTIR stretching Si–O pulse at 1150/cm (Fig. 2(b)). The obtained PXRD diffractogram confirmed that the ULBC has a heterogeneous surface (Liu et al., 2012), and it corroborated with the SEM images, as shown in Fig. 1.

The PXRD diffractogram of soil and amended soil are displayed in Fig. 3 (b) and (c). More peaks of quartz were observed at 2θ of 20.8°, 26.7°, 36.5°, 42.3°, 45.9°, 50.1°, 54.8°, 60.1°, and 67.6° (Amalero et al., 2003). Also, few minor peaks appeared at 2θ of 18.3, and 12.3 and 39.6 referred to illite clay mineral and kaolinite, respectively (Amalero et al., 2003). The FTIR pulses confirmed the occurrence of quartz and kaolinite

Table 1
Physicochemical properties of soil, ULBC, and amended soil.

Samples	pH	Conductivity	CEC cmol/kg	Sand %	Silt %	Clay %	USDA class
Soil	6.39 ± 0.01	18.41 ± 0.04 μS/cm	3.84 ± 0.01	85	05	10	Loamy sand
			Ash%	**Moisture%**	**Resident matter%**	**Mobile matter%**	
ULBC	10.26 ± 0.03	3.39 ± 0.01 mS/cm	38.36 ± 0.42	4.68 ± 0.20	13.15 ± 0.47	43.62 ± 0.39	
ULBC amended soil	7.86 ± 0.03	396.13 ± 0.25 μS/cm	2.43 ± 0.014	2.35 ± 0.006	88.97 ± 0.012	6.25 ± 0.021	

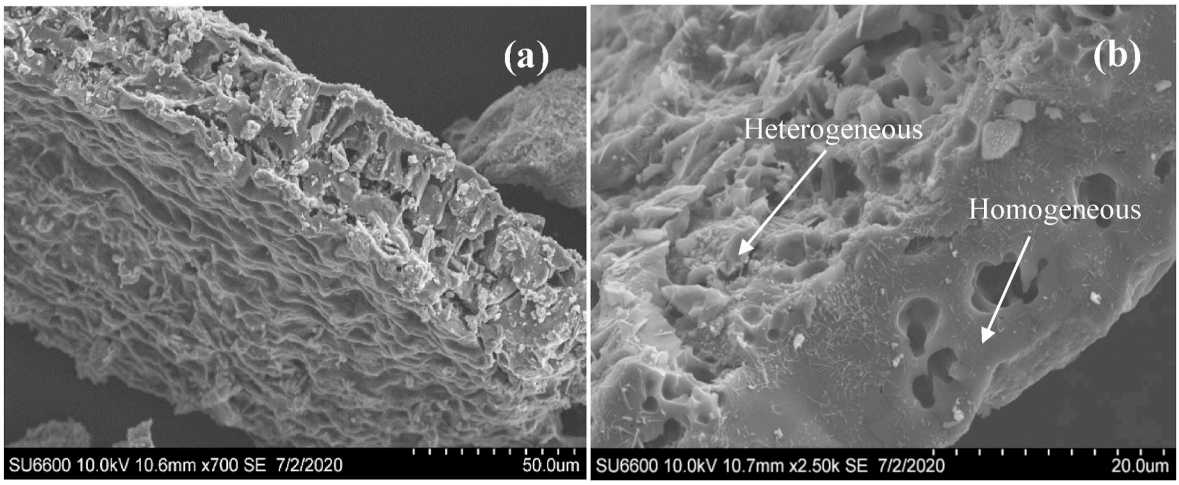

Fig. 1. The SEM images of ULBC at different magnifications of (a) X700 and (b) X2500.

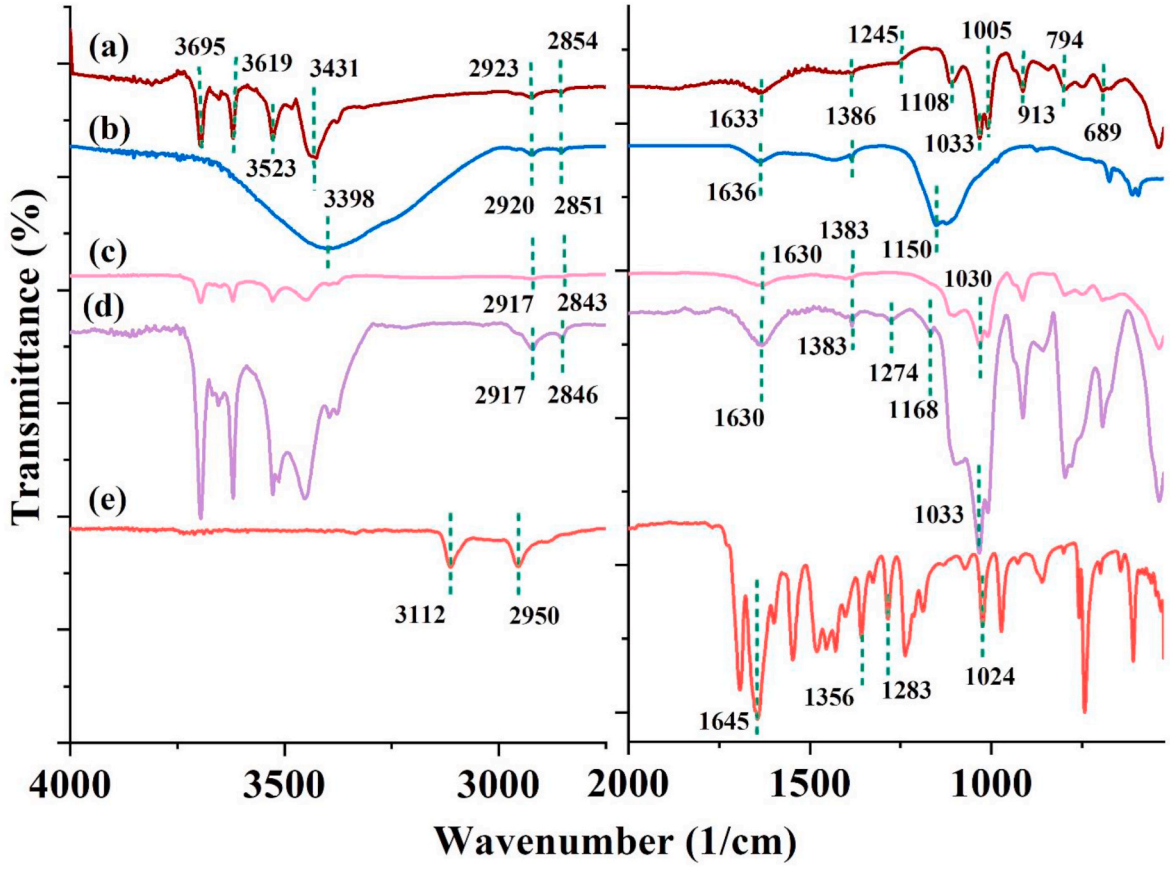

Fig. 2. The FTIR spectra of (a) soil, (b) ULBC, (c) CFN-soil, (d) CFN-amended soil, and (e) CFN.

in the soil at 1108, 1005, and 913/cm, which referred to Si–O–Si, Si–O, and Al–OH functional groups (Xing et al., 2019).

3.2. Optimizing the effective pH

The pH edge experiment shown in Fig. 4 illustrates the variation of adsorption capacity of CFN by soil and ULBC-soil as a function of pH. Soil exhibited limited adsorption of CFN all the pHs indicating a high probability of transport of CFN. The addition of 2.5% ULBC to the soil has shown a significant increase (4-fold) in the CFN retention of soil Fig. 4(a). The distribution coefficient (*Kd*) of CFN in the soil and amended soil displayed a similar trend to the adsorption capacity, shown in Fig. 4(b). The *Kd* of CFN in soil and amended soil was 0.005 and 0.05 L/g, respectively. The application of ULBC to the soil increased the *Kd* ten-fold at pH 4 and 25 °C. As reported by Beltrame et al. (2018), the neutral form of CFN molecule dominated in the acidic pH < 5.5, while anionic species dominated in the pH > 5.5. The pHzpc of soil and ULBC amendment was determined as 6.099 and 7.368, respectively shown in Fig. 4 (c). The dominant surface charge of adsorbents was positive when pHzpc > solution pH, whereas negative charges dominate when the pHzpc < solution pH (Beltrame et al., 2018). In soil, the adsorption of neutral and/or cationic form of CFN was high by the

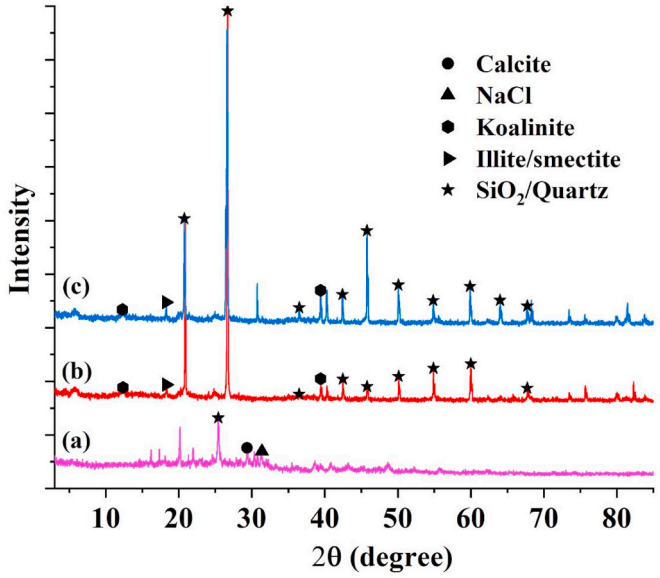

Fig. 3. The PXRD diffractogram of (a) ULBC, (b) soil, and (c) amended soil.

positively charged soil below pH 6, indicating the contribution of non-electrostatic interaction. Similar pattern was observed in the study for CFN interaction with water hyacinth biochar (Ngeno et al., 2016). On the whole, environmental pHs (pH 4–7) demonstrated insignificant differences for CFN adsorption.

3.3. Effect of the initial concentration of CFN

The retention behavior of CFN in unamended soil and ULBC amended soil is plotted in Fig. 5 (a) and (b), as a function of equilibrium concentration along with their well-fitted isotherm models. The adsorption capacities of CFN by both unamended and amended soil as increased by raising the CFN concentration at the optimum pH of 4 and room temperature of 25 °C. The addition of 2.5% ULBC demonstrated high retention of CFN, as shown in Fig. 5. In the acidic pH, the soil organic matter can compete with the CFN molecule during the adsorption process. In the case of amendment, the application of ULBC to the soil can provide additional affinity sites to the CFN molecules (Vithanage et al., 2014). Hence, the ULBC amended soil exhibited significant attributes (2-fold) to the CFN under the experimental conditions.

The well-fitted isotherm models were identified based on the determination coefficient (R^2), error, and Chi^2 values. The predicted isotherm parameters are listed in Table 2. The unamended soil was fitted well with the Temkin isotherm followed by Langmuir isotherm and Freundlich isotherm, whereas, in amended soil, it was Langmuir isotherm followed by Freundlich isotherm and Temkin isotherm. Generally, the Temkin isotherm describes that the heat of adsorption would drop linearly due to the adsorbent-adsorbate interaction (Mayakaduwa et al., 2016). The Temkin parameter values of A_T and B of unamended soil were 0.1124 L/mg and 0.0819 J/mol manifests that the adsorption of CFN onto unamended soil-driven due to the weak forces such as van der Waals interaction, hydrogen bonding, charge transfer, and π–π and π–n interaction (Keerthanan et al., 2020b).

The Langmuir isotherm states that the adsorption takes place through mono-layer coverage, and also it assumed the energy of active sites on the homogeneous surface is equally distributed, wherein the adsorption process terminated when the active sites saturated (de Franco et al., 2018; Scheufele et al., 2016). The mono-layer maximum adsorption capacity (Q_{max}) of unamended soil and amended soil were 0.417 and 0.815 mg/g respectively, indicating that the addition of ULBC to the soil enhanced the retention of CFN in the soil with involving of strong chemical interaction such as electrostatic interaction between CFN and ULBC amended soil. The Langmuir separation factor (R_L) was calculated using equation (5) and it was plotted as the function of CFN initial concentration in Fig. 5 (c) and (d). Generally, the R_L value indicated the favorability: $R_L = 0$ indicates the adsorption is irreversible, while $0 < R_L < 1$ indicates the adsorption is favorable. The $R_L = 1$, the process is linear, whereas $R_L > 1$ indicates the unfavorable adsorption (Stromer et al., 2018). The R_L values of both unamended and amended soils were less than one; Fig. 5 (c) and (d) suggested the adsorption was favorable and it was exponentially decreased between 0.9 and 0.1 with the increasing of the initial CFN concentration suggesting that the CFN adsorption becomes more favorable at high concentration (Stromer et al., 2018).

The Freundlich isotherm model also adequately fitted with experimental results from both unamended and amended soil based on the R^2 value of 0.9206 and 0.9528, respectively. The Freundlich isotherm describes that the adsorption takes place at a heterogeneous surface of the adsorbent, wherein the energy of active sites are distributed exponentially (Araújo et al., 2018). The adsorption intensity (n) of unamended and amewasd soil were 0.62 and 0.34 respectively that indicating, the adsorption of CFN by unamended and amended soil was favorable (Keerthanan et al., 2020a).

3.4. Retention potential of CFN onto the soil

The passage of CFN through the unamended and amended soil was shown in Fig. 6. Initially, the columns were washed with ultra-pure water. Thereafter, the CFN solution was injected, followed by leaching with ultra-pure water. The retention of CFN in unamended soil was subordinated. The retained mass of CFN in unamended soil was estimated as 0.254 mg equaling to 15.5% retained from the initially fed CFN mass. This indicates, low retention potential of CFN in loamy sand. The addition of 2.5% ULBC to the soil increased the retention mass of CFN to 1.399 mg, which equates to about 85.5% of the initially injected CFN

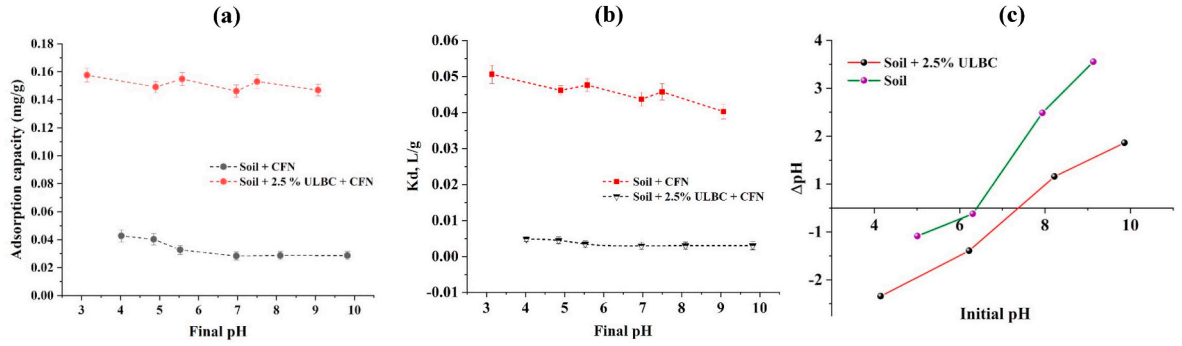

Fig. 4. The adsorption capacity (a), distribution coefficient (b) of CFN by soil and amended soil as a function of final pH at 25 °C, and zero-point charge (pHzpc) of soil and ULBC amendment (c).

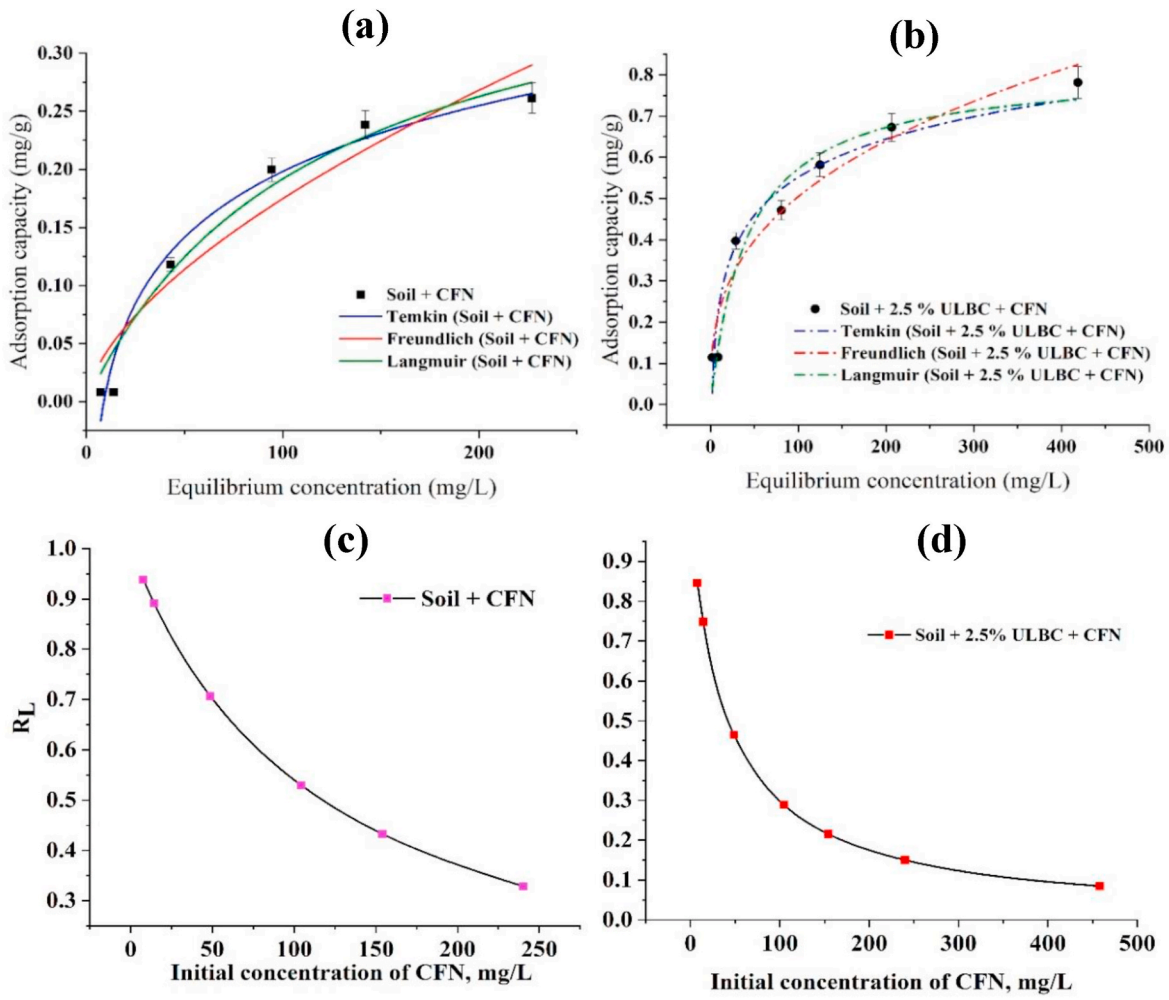

Fig. 5. The fitted adsorption isotherms models of (a) soil and (b) amended soil, and Langmuir model separation factor in (c) soil and (d) amended soil as a function of the initial concentration of CFN.

Table 2
The parameters obtained from adsorption isotherm models.

Samples	Isotherm models					
	Freundlich model		Langmuir model		Temkin model	
Soil	K_f	0.0101	k_L	0.0085	A_T	0.1124
	n	0.6181	Q_{max}	0.4168	b	30255
	Chi^2	0.0013	Chi^2	5.11861E-4	B	0.0819
	R^2	0.9206	R^2	0.9676	Chi^2	4.19806E-4
					R^2	0.9734
ULBC-soil amendment	K_f	0.1038	k_L	0.0236	A_T	0.6234
	n	0.3433	Q_{max}	0.8147	b	18558
	Chi^2	0.0038	Chi^2	0.0035	B	0.1335
	R^2	0.9528	R^2	0.9570	Chi^2	0.0048
					R^2	0.9412

mass.

The ratio of CFN concentration in effluent and influent solution (C/C_o) was estimated to understand the CFN retention capacity in soil. Initially, no CFN was detected from both unamended and amended soil when the two-pore volume of ultra-pure water feed. Thereafter, the ratio of C/C_o was rapidly increased to a maximum value of 0.77 when 8 pore volumes of CFN solution injected, indicates the transport of CFN in the

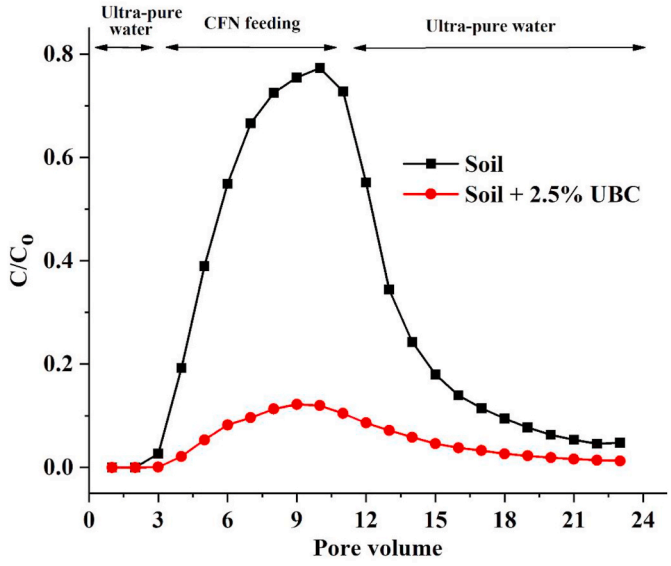

Fig. 6. The ratio of outlet and inlet CFN concentration in soil and amended the soil-filled column as a function of pore volume.

natural loamy sand was high. Finally, C/C_o was decreased exponentially to 0.046 after feeding the ultra-pure water, which manifested the CFN retention was less in the loamy sand.

The C/C_o of amendment soil also followed a similar trend as the unamended soil, shown in Fig. 6. However, low transport of CFN was recorded with maximum C/C_o of 0.12, indicates the high retention of CFN in the ULBC amended loamy sand. A similar trend of observations in the retention of sulfamethazine in invasive plant biochar amended soil was reported by Vithanage et al. (2014).

The column experiment data have agreed with the results of the batch adsorption experiment. However, the experimental conditions for both batch and column experiments were varied. The batch experiments were conducted at a pH of 4, while soil column experiments were carried out at pH ranging from 6 to 8. According to pH edge results (Fig. 4), the CFN adsorption by unamended soil was pH-dependent, whereas CFN sorption by amended biochar was pH-independent. The application of ULBC to the loamy sand has provided additional adsorption active sites, which enhanced the retention of CFN in soil than unamended soil.

The Thomas and Yoon-Nelson models were fitted with column experiment results at an influent CFN concentration of 10.225 mg/L and an average flow rate of 1.25 mL/min through the columns with a height of 10 cm and diameter of 2.7 cm. The linear plots of Thomas and Yoon-Nelson models are provided in Fig. 7 (a) and (b) respectively. The linear regression lines of both models were moderately fitted with the experimental results and the predicted parameters are tabulated in Table 3.

The Thomas model showed a negative linear correlation, whereas the Yoon-Nelson model exhibited a positive linear correlation based on Pearson's R (Table 3). The Thomas rate constant was decreased while the Thomas uptake capacity was 2-fold increased with 2.5% of ULBC to the soil. The application of 2.5% of ULBC to the soil increased the τ value while decreased the K_{YN}. The predicted q_{YN} (uptake capacity corresponding to Yoon-Nelson) also increased 2-fold with the addition of 2.5% of ULBC (Table 3). These changes might be due to the surface reaction between CFN and amendment (Patel, 2019).

3.5. Toxicity characteristic leaching procedure (TCLP) extraction

The TCLP experiments were conducted on the contaminated soil from the columns. The results revealed the extraction of CFN from the loamy sand type soil was <2E-5 mg, and this was calculated based on the limit of detection (0.001 mg/L) to 20 mL solution. The dissolution of CFN was estimated as soil 8.2E-4 mg from amended soil. It is assumed that the CFN binding with amended and unamended soil is through mixed chemical and physical sorption mechanisms, which corroborate with isotherm experiment results. The best-fitted adsorption isotherm of Temkin and Langmuir models for unamended soil and Langmuir and Freundlich isotherm models for amended soil also suggested the mixed adsorption mechanisms. However, it shows that the physisorbed CFN is limited, indicating a strong bond formation with the seaweed biochar.

Table 3
Predicted column models' parameters for CFN adsorption.

Column	Slope	Intercept	Pearson's R	R^2	Parameters	
Yoon-Nelson model						
Soil column	0.027	−3.5	0.94	0.89	K_{YN}	0.027
					τ	130
					q_{YN}	0.029
ULBC amended column	0.021	−5.5	0.91	0.83	K_{YN}	0.021
					τ	262
					q_{YN}	0.059
Thomas model						
Soil column	−0.027	3.5	−0.94	0.89	k_{TH}	2.64E-3
					q_{TH}	29.32
ULBC amended column	−0.017	4.9	−0.88	0.77	k_{TH}	1.66E-3
					q_{TH}	65.20

3.6. Adsorption comparison

The CFN adsorption onto the soil was previously investigated in Richards et al. (2017) and Zhang et al. (2013). The untreated and ozone-treated soil were used in the CFN adsorption from septic tank effluent, and the distribution coefficient (Kd) of CFN in both soils was 22.16 and 19.72 cm^3/g (Richards et al., 2017). Similarly, the Kd was obtained for sediment, silt-loam, and sand-soil was reported as 5.01, 5.78, and 3.17 cm^3/g (Zhang et al., 2013). The present study found a lower Kd (4.83 cm^3/g) for CFN adsorption in unamended soil compared with previous studies (Table 4 (a)). However, the Kd was increased up to 50.62 cm^3/g when 2.5% of ULBC amended with the same soil. Also, Table 4 (b) is summarized few recent studies which performed adsorptive removal of CFN by different types of biochar and the role of seaweeds biochar in the removal of organic and inorganic contaminants from the aqueous solution reviewed in Table 4 (C). The conversion of seaweeds into a valuable product to mitigate emerging pollutants and

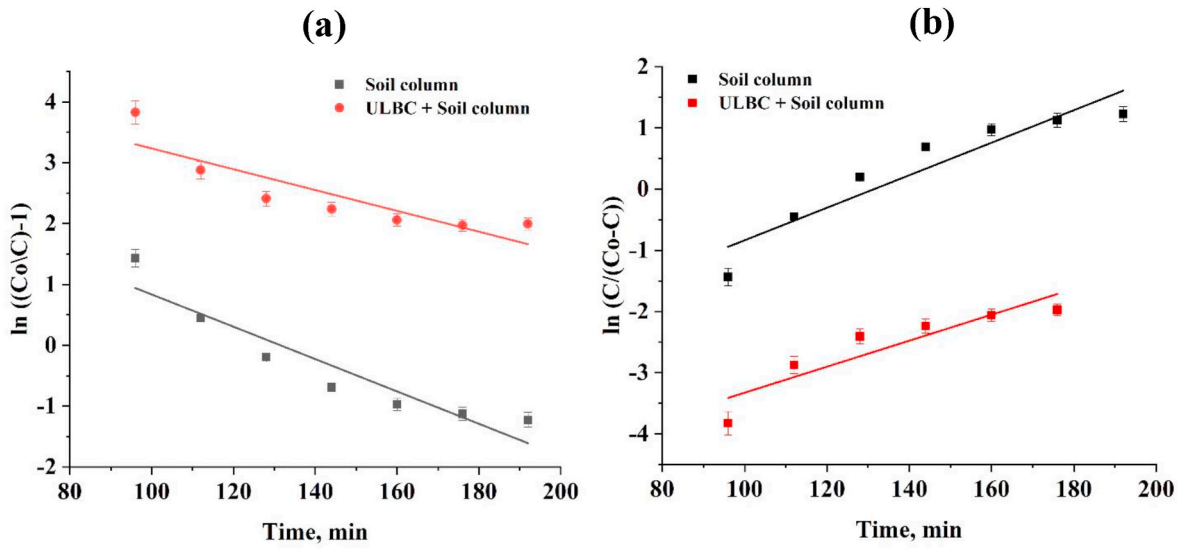

Fig. 7. The linear fitted plots of Thomas model (a) and Yoon-Nelson model.

Table 4
Comparison of CFN adsorption on soil and biochar, and role of seaweed biochar in the removal of contaminants.

Adsorbent	Physicochemical properties	Contaminants	Media	Maximum adsorption capacity (*Qmax*)/Distribution coefficient (*Kd*)	References
(a) Comparison of CFN adsorption in soil				*Kd* (cm^3/g)	
Untreated soil	pH: 5.98	Caffeine	Septic tank effluent	22.16	Richards et al. (2017)
Ozone treated soil	moisture content: 16.28% Clay particle size: 7.35%			19.72	
Unamended soil	pH: 6.39 EC:18.41 μS/cm CEC: 3.84 cmol/kg	Caffeine	Caffeine contaminated water	2.97–4.83	Present study
ULBC amended soil	pH: 7.86 EC: 396.13 μS/cm Moisture content: 2.35%			40.26–50.62	
Sediment	pH: 7.8 OC: 3.22% OM: 5.58%	Caffeine	Caffeine contaminated water	5.01	Zhang et al. (2013)
Silt-loam	pH: 7.92 OC: 3.67% OM:6.23%			5.78	
Sand-soil	pH: 7.85 OC: 2.89% OM:4.91%			3.17	
(b) Performance of biochar in CFN adsorption				*Qmax* (*mg /g*)	
Tea waste biochar	SA: 576 PV: 0.1091 PT: 700 Activation: Steam	Caffeine	Synthetic wastewater	15.4	Keerthanan et al. (2020a)
Pine tree needles biochar	PT: 650	Caffeine	Synthetic wastewater Real wastewater	5.35 1.41	Anastopoulos et al. (2020)
Gliricidia sepium biochar	pH: 10.1 EC: 1.7 dS/m SA: 216.4 PV: 0.1097 PT: 700	Caffeine	Synthetic wastewater	16.26	Keerthanan et al. (2020b)
(c) Seaweed biochar in organic and inorganic contaminant removal				*Qmax* (*mg /g*)	
Gracilaria Rhodophyta biochar (red algae)	pH: 7.6 moisture content: 5.85 Ash content: 2.39 SA: 319.47 OM: 824.77 g/kg CEEC: 6.63 cmol/kg PV: 0.426 PT: 450	Aluminum Fluoride	Synthetic wastewater	44.5 2.1	Naga Babu et al. (2020)
N-doped *Ulva prolifera* biochar	SA: 25.43 PT: 200	Bisphenol	Synthetic wastewater	33.3	Lu et al. (2017)
Sargassum sp biochar	PT: 600 Carbon content: increased from 22.9 to 37.2% Oxygen content: increased from 24.7 to 27.8%	Tetracycline Cefradine	Synthetic wastewater	128.1 61.7	Song et al. (2019)
Gelidiella acerosa biochar	SA: 926.39 PV: 0.57 PT: 800	Methylene blue	Synthetic wastewater	512.67	Ahmed et al. (2019)
Ulva reticulata biochar	PT: 300	Arsenic (V)	Synthetic wastewater	7.67	Senthilkumar et al. (2020)

EC: Electrical conductivity SA: Surface area (m^2/g), PV: Pore volume (cm^3/g), OC: Organic carbon content, OM: Organic matter content, PT: Pyrolysis temperature (°C), CEC: Cation exchange capacity.

improve the soil fertility is timely needed since a massive growth of them around the global seaside.

4. Conclusions

The transport and retention affinity of CFN in soil and seaweed biochar amended soil were accessed viabatch, column, and TCLP experiments. The ULBC was derived at 500 °C, and it was characterized using FTIR, SEM, and PXRD. The experimental soil was characterized as loamy sand that contains organic matter, quartz, and kaolinite minerals, which was concluded based on the FTIR and PXRD analysis. The SEM images revealed that the ULBC possessed a heterogeneous and homogeneous surface. The CFN retention in the unamended soil is gently dependent on the pH. The selected loamy sand soil has shown a minimal adsorption affinity with CFN molecules at pH 4.0 and 25 °C. The addition of 2.5% of ULBC to the soil enhanced the retention affinity significantly. The CFN adsorption by amended soil was hardly dependent on the pH. The column experiments concluded that the transport of CFN in loamy sandy soil was high, and it was limited, with the addition of 2.5% of ULBC to the loamy sandy soil. The adsorption isotherm models postulated the CFN adsorption onto the unamended soil through non-electrostatic interaction, whereas in amended soil via electrostatic interaction. The uptake capacities predicted from the Thomas and Yoon-Nelson models of the soil have improved with 2.5% of ULBC. Overall,

the application of ULBC to the soil can decrease the transport of CFN to the aquatic environment, reducing the risk to the human and environment. However, the current study investigated the CFN retention and transport in an amended and unamended soil using a mono-contaminate system. Therefore, a future study should be carried out in a multi-contaminants system under ambient environmental conditions. The application of biochar to the agricultural soil can be reduced the plant uptake of CFN. Therefore, the studies on plant uptake of CFN with and without biochar amendment are future needs.

Author statement

S. Keerthanan: Experimentation, data interpretation, data validation, writing the first draft Chaminda Gunarardane: Data validation, Reviewing and editing Thiruchenduran Somasundaram: Experimentation, Validation and reviewing Tharuka Jayampathi: Reviewing and editing Chamila Jayasinghe: Supervision, Reviewing and editing Meththika Vithanage: Conceptualization, Supervision, Project administration, Funding acquisition, writing-reviewing and editing

Declaration of competing interest

The authors declare that they have no known competing financial interests or personal relationships that could have appeared to influence the work reported in this paper.

Acknowledgment

Authors acknowledge financial assistant (Grant No: ASP/01/RE/SCI/2018-65) provided by the Research Council, University of Sri Jayewardenepura, Sri Lanka.

References

Ahmad, M., Lee, S.S., Rajapaksha, A.U., Vithanage, M., Zhang, M., Cho, J.S., Lee, S.E., Ok, Y.S., 2013. Trichloroethylene adsorption by pine needle biochars produced at various pyrolysis temperatures. Bioresour. Technol. 143, 615–622. https://doi.org/10.1016/j.biortech.2013.06.033.

Ahmad, M., Rajapaksha, A.U., Lim, J.E., Zhang, M., Bolan, N., Mohan, D., Vithanage, M., Lee, S.S., Ok, Y.S., 2014. Biochar as a sorbent for contaminant management in soil and water: a review. Chemosphere 99, 19–33. https://doi.org/10.1016/j.chemosphere.2013.10.071.

Ahmadi, S., Gitipour, S., Marzani, S., Mehrdadi, N., 2016. Microsilica-cement stabilization of organic contaminated soil: leaching behaviour of polycyclic aromatic hydrocarbons. Curr. World Environ. 11, 20–27. https://doi.org/10.12944/CWE.11.1.03.

Ahmed, M.J., Okoye, P.U., Hummadi, E.H., Hameed, B.H., 2019. High-performance porous biochar from the pyrolysis of natural and renewable seaweed (*Gelidiella acerosa*) and its application for the adsorption of methylene blue. Bioresour. Technol. 278, 159–164. https://doi.org/10.1016/j.biortech.2019.01.054.

Álvarez-Torrellas, S., Rodríguez, A., Ovejero, G., Gómez, J.M., García, J., 2016. Removal of caffeine from pharmaceutical wastewater by adsorption: influence of NOM, textural and chemical properties of the adsorbent. Environ. Technol. 37, 1618–1630. https://doi.org/10.1080/09593330.2015.1122666.

Álvarez, S., Ribeiro, R.S., Gomes, H.T., Sotelo, J.L., García, J., 2015. Synthesis of carbon xerogels and their application in adsorption studies of caffeine and diclofenac as emerging contaminants. Chem. Eng. Res. Des. 95, 229–238. https://doi.org/10.1016/j.cherd.2014.11.001.

Amalero, E.G., Ingua, G.L., Erta, G.B., Emanceau, P.L., 2003. Review article Methods for studying root colonization by introduced. Agronomie 23, 407–418. https://doi.org/10.1051/agro.

Anastopoulos, I., Katsouromalli, A., Pashalidis, I., 2020. Oxidized biochar obtained from pine needles as a novel adsorbent to remove caffeine from aqueous solutions. J. Mol. Liq. 304, 112661. https://doi.org/10.1016/j.molliq.2020.112661.

Araújo, C.S.T., Almeida, I.L.S., Rezende, H.C., Marcionilio, S.M.L.O., Léon, J.J.L., de Matos, T.N., 2018. Elucidation of mechanism involved in adsorption of Pb(II) onto lobeira fruit (*Solanum lycocarpum*) using Langmuir, Freundlich and Temkin isotherms. Microchem. J. 137, 348–354. https://doi.org/10.1016/j.microc.2017.11.009.

Atugoda, T., Wijesekara, H., Werellagama, D.R.I.B., Jinadasa, K.B.S.N., Bolan, N.S., Vithanage, M., 2020. Adsorptive interaction of antibiotic ciprofloxacin on polyethylene microplastics: implications for vector transport in water. Environ. Technol. Innov. 19, 100971. https://doi.org/10.1016/j.eti.2020.100971.

Balakrishna, K., Rath, A., Praveenkumarreddy, Y., Guruge, K.S., Subedi, B., 2017. A review of the occurrence of pharmaceuticals and personal care products in Indian water bodies. Ecotoxicol. Environ. Saf. 137, 113–120. https://doi.org/10.1016/j.ecoenv.2016.11.014.

Bandara, T., Herath, I., Kumarathilaka, P., Seneviratne, M., Seneviratne, G., Rajakaruna, N., Vithanage, M., Ok, Y.S., 2017. Role of woody biochar and fungal-bacterial co-inoculation on enzyme activity and metal immobilization in serpentine soil. J. Soils Sediments 17, 665–673. https://doi.org/10.1007/s11368-015-1243-y.

Beltrame, K.K., Cazetta, A.L., de Souza, P.S.C., Spessato, L., Silva, T.L., Almeida, V.C., 2018. Adsorption of caffeine on mesoporous activated carbon fibers prepared from pineapple plant leaves. Ecotoxicol. Environ. Saf. 147, 64–71. https://doi.org/10.1016/j.ecoenv.2017.08.034.

Ben-Ali, S., Jaouali, I., Souissi-Najar, S., Ouederni, A., 2017. Characterization and adsorption capacity of raw pomegranate peel biosorbent for copper removal. J. Clean. Prod. 142, 3809–3821. https://doi.org/10.1016/j.jclepro.2016.10.081.

Choi, Y., Kim, K., Kim, D., Moon, H. bang, Jeon, J., 2020. Ny-Ålesund-oriented organic pollutants in sewage effluent and receiving seawater in the Arctic region of Kongsfjorden. Environ. Pollut. 258, 113792. https://doi.org/10.1016/j.envpol.2019.113792.

de Franco, M.A.E., de Carvalho, C.B., Bonetto, M.M., de Pelegrini Soares, R., Féris, L.A., 2018. Diclofenac removal from water by adsorption using activated carbon in batch mode and fixed-bed column: isotherms, thermodynamic study and breakthrough curves modeling. J. Clean. Prod. 181, 145–154. https://doi.org/10.1016/j.jclepro.2018.01.138.

Dodgen, L.K., Li, J., Wu, X., Lu, Z., Gan, J.J., 2014. Transformation and removal pathways of four common PPCP/EDCs in soil. Environ. Pollut. 193, 29–36. https://doi.org/10.1016/j.envpol.2014.06.002.

Gokulan, R., Prabhu, G.G., Jegan, J., 2019. Remediation of complex remazol effluent using biochar derived from green seaweed biomass. Int. J. Phytoremediation 21, 1179–1189. https://doi.org/10.1080/15226514.2019.1612845.

Gunarathne, V., Senadeera, A., Gunarathne, U., Biswas, J.K., Almaroai, Y.A., Vithanage, M., 2020. Potential of biochar and organic amendments for reclamation of coastal acidic-salt affected soil. Biochar 2, 107–120. https://doi.org/10.1007/s42773-020-00036-4.

Guruge, K.S., Goswami, P., Tanoue, R., Nomiyama, K., Wijesekara, R.G.S., Dharmaratne, T.S., 2019. First nationwide investigation and environmental risk assessment of 72 pharmaceuticals and personal care products from Sri Lankan surface waterways. Sci. Total Environ. 690, 683–695. https://doi.org/10.1016/j.scitotenv.2019.07.042.

Hu, S., Zhang, Y., Shen, G., Zhang, H., Yuan, Z., Zhang, W., 2019. Adsorption/desorption behavior and mechanisms of sulfadiazine and sulfamethoxazole in agricultural soil systems. Soil Tillage Res. 186, 233–241. https://doi.org/10.1016/j.still.2018.10.026.

Jain, S., Srivastava, A.S., Verma, R.P., Maggu, G., 2019. Caffeine addiction: need for awareness and research and regulatory measures. Asian J. Psychiatr. 41, 73–75. https://doi.org/10.1016/j.ajp.2017.01.008.

Jayawardhana, Y., Mayakaduwa, S.S., Kumarathilaka, P., Gamage, S., Vithanage, M., 2019. Municipal solid waste-derived biochar for the removal of benzene from landfill leachate. Environ. Geochem. Health 41, 1739–1753. https://doi.org/10.1007/s10653-017-9973-y.

Jiang, Z., Hu, D., 2019. Molecular mechanism of anionic dyes adsorption on cationized rice husk cellulose from agricultural wastes. J. Mol. Liq. 276, 105–114. https://doi.org/10.1016/j.molliq.2018.11.153.

Keerthanan, S., Bhatnagar, A., Mahatantila, K., Jayasinghe, C., Ok, Y.S., Vithanage, M., 2020a. Engineered tea-waste biochar for the removal of caffeine, a model compound in pharmaceuticals and personal care products (PPCPs), from aqueous media. Environ. Technol. Innov. 19, 100847. https://doi.org/10.1016/j.eti.2020.100847.

Keerthanan, S., Jayasinghe, C., Biswas, J.K., Vithanage, M., 2020. Pharmaceutical and Personal Care Products (PPCPs) in the environment: plant uptake, translocation, bioaccumulation, and human health risks. Crit. Rev. Environ. Sci. Technol. 1–38. https://doi.org/10.1080/10643389.2020.1753634.

Keerthanan, S., Rajapaksha, S.M., Trakal, L., Vithanage, M., 2020b. Caffeine removal by *Gliricidia sepium* biochar: influence of pyrolysis temperature and physicochemical properties. Environ. Res. 109865. https://doi.org/10.1016/j.envres.2020.109865.

Kim, P., Johnson, A., Edmunds, C.W., Radosevich, M., Vogt, F., Rials, T.G., Labbé, N., 2011. Surface functionality and carbon structures in lignocellulosic-derived biochars produced by fast pyrolysis. Energy Fuels 25, 4693–4703. https://doi.org/10.1021/ef200915s.

Kleywegt, S., Payne, M., Raby, M., Filippi, D., Ng, C.F., Fletcher, T., 2019. The final discharge: quantifying contaminants in embalming process effluents discharged to sewers in ontario, Canada. Environ. Pollut. 252, 1476–1482. https://doi.org/10.1016/j.envpol.2019.06.036.

Korekar, G., Kumar, A., Ugale, C., 2019. Occurrence, fate, persistence and remediation of caffeine: a review. Environ. Sci. Pollut. Res. 1–19. https://doi.org/10.1007/s11356-019-06998-8.

Kosma, C.I., Lambropoulou, D.A., Albanis, T.A., 2014. Investigation of PPCPs in wastewater treatment plants in Greece: occurrence, removal and environmental risk assessment. Sci. Total Environ. 466–467, 421–438. https://doi.org/10.1016/j.scitotenv.2013.07.044.

Li, C., Chen, J., Wang, J., Ma, Z., Han, P., Luan, Y., Lu, A., 2015. Occurrence of antibiotics in soils and manures from greenhouse vegetable production bases of Beijing, China and an associated risk assessment. Sci. Total Environ. 521–522, 101–107. https://doi.org/10.1016/j.scitotenv.2015.03.070.

Li, J., Yu, G., Pan, L., Li, C., You, F., Xie, S., Wang, Y., Ma, J., Shang, X., 2018. Study of ciprofloxacin removal by biochar obtained from used tea leaves. J. Environ. Sci. (China) 73, 20–30. https://doi.org/10.1016/j.jes.2017.12.024.

Li, S., He, B., Wang, J., Liu, J., Hu, X., 2020a. Risks of caffeine residues in the environment: necessity for a targeted ecopharmacovigilance program. Chemosphere 243. https://doi.org/10.1016/j.chemosphere.2019.125343.

Li, X., Wang, C., Tian, J., Liu, J., Chen, G., 2020b. Comparison of adsorption properties for cadmium removal from aqueous solution by Enteromorpha prolifera biochar modified with different chemical reagents. Environ. Res. 186, 109502. https://doi.org/10.1016/j.envres.2020.109502.

Liu, Xianjing, Liang, C., Liu, Xiaohui, Zhao, F., Han, C., 2020. Occurrence and human health risk assessment of pharmaceuticals and personal care products in real agricultural systems with long-term reclaimed wastewater irrigation in Beijing, China. Ecotoxicol. Environ. Saf. 190, 110022. https://doi.org/10.1016/j.ecoenv.2019.110022.

Liu, Y., Zhao, X., Li, J., Ma, D., Han, R., 2012. Characterization of bio-char from pyrolysis of wheat straw and its evaluation on methylene blue adsorption. Desalin. Water Treat. 46, 115–123. https://doi.org/10.1080/19443994.2012.677408.

Lopez-Sanchez, R.D.C., Lara-Diaz, V.J., Aranda-Gutierrez, A., Martinez-Cardona, J.A., Hernandez, J.A., 2018. HPLC method for quantification of caffeine and its three major metabolites in human plasma using fetal bovine serum matrix to evaluate prenatal drug exposure. J. Anal. Methods Chem. https://doi.org/10.1155/2018/2085059, 2018.

Lu, J., Zhang, C., Wu, J., Luo, Y., 2017. Adsorptive removal of bisphenol A using N-doped biochar made of Ulva prolifera. Water Air Soil Pollut. 228, 1–9. https://doi.org/10.1007/s11270-017-3516-0.

Luo, Y., Guo, W., Ngo, H.H., Nghiem, L.D., Hai, F.I., Zhang, J., Liang, S., Wang, X.C., 2014. A review on the occurrence of micropollutants in the aquatic environment and their fate and removal during wastewater treatment. Sci. Total Environ. 473–474, 619–641. https://doi.org/10.1016/j.scitotenv.2013.12.065.

Ma, L., Liu, Y., Zhang, J., Yang, Q., Li, G., Zhang, D., 2018. Impacts of irrigation water sources and geochemical conditions on vertical distribution of pharmaceutical and personal care products (PPCPs) in the vadose zone soils. Sci. Total Environ. 626, 1148–1156. https://doi.org/10.1016/j.scitotenv.2018.01.168.

Madikizela, L.M., Ncube, S., Chimuka, L., 2018. Uptake of pharmaceuticals by plants grown under hydroponic conditions and natural occurring plant species: a review. Sci. Total Environ. 636, 477–486. https://doi.org/10.1016/j.scitotenv.2018.04.297.

Manyà, J.J., 2012. Pyrolysis for biochar purposes: a review to establish current knowledge gaps and research needs. Environ. Sci. Technol. 46, 7939–7954. https://doi.org/10.1021/es301029g.

Martínez-López, S., Sarriá, B., Baeza, G., Mateos, R., Bravo-Clemente, L., 2014. Pharmacokinetics of caffeine and its metabolites in plasma and urine after consuming a soluble green/roasted coffee blend by healthy subjects. Food Res. Int. 64, 125–133. https://doi.org/10.1016/j.foodres.2014.05.043.

Massey, L.K., Sutton, R.A.L., 2004. Acute caffeine effects on urine composition and calcium kidney stone risk in calcium stone formers. J. Urol. 172, 555–558. https://doi.org/10.1097/01.ju.0000129413.87024.5c.

Mayakaduwa, S.S., Vithanage, M., Karunarathna, A., Mohan, D., Ok, Y.S., 2016. Interface interactions between insecticide carbofuran and tea waste biochars produced at different pyrolysis temperatures. Chem. Speciat. Bioavailab. 28, 110–118. https://doi.org/10.1080/09542299.2016.1198928.

Michalak, I., Baśladyńska, S., Mokrzycki, J., Rutkowski, P., 2019. Biochar from a freshwater macroalga as a potential biosorbent for wastewater treatment. Water (Switzerland) 11, 4–6. https://doi.org/10.3390/w11071390.

Miossec, C., Lanceleur, L., Monperrus, M., 2019. Multi-residue analysis of 44 pharmaceutical compounds in environmental water samples by solid-phase extraction coupled to liquid chromatography-tandem mass spectrometry. J. Separ. Sci. 42, 1853–1866. https://doi.org/10.1002/jssc.201801214.

Naga Babu, A., Srinivasa Reddy, D., Suresh Kumar, G., Ravindhranath, K., Krishna Mohan, G.V., 2020. Sequential synergetic sorption analysis of *Gracilaria Rhodophyta* biochar toward aluminum and fluoride: a statistical optimization approach. Water Environ. Res. 92, 880–898. https://doi.org/10.1002/wer.1283.

Ngeno, E.C., Francis, O., Lilechi Danstone, B., Victor Odhiambo, S., Selly Jemutai, K., 2016. Adsorption of caffeine and ciprofloxacin onto pyrolitically derived water hyacinth biochar: isothermal, kinetic and thermodynamic studies. J. Chem. Chem. Eng. 10 https://doi.org/10.17265/1934-7375/2016.04.006.

Ornaf, R.M., Dong, M.W., 2005. Key concepts of HPLC in pharmaceutical analysis. Separ. Sci. Technol. 6, 19–45. https://doi.org/10.1016/S0149-6395(05)80046-7.

Patel, H., 2019. Fixed-bed column adsorption study: a comprehensive review. Appl. Water Sci. 9, 1–17. https://doi.org/10.1007/s13201-019-0927-7.

Pavia, D.L., Lampman, G.M., Kriz, G.S., 2001. Introduction to Spectroscopy - A Guide for Students of Organic Chemistry, Third. ed. Thomson Learning, Inc., USA.

Pham, V.T.T., Ismail, T., Mishyna, M., Appiah, K.S., Oikawa, Y., Fujii, Y., 2019. Caffeine: the allelochemical responsible for the plant growth inhibitory activity of Vietnamese tea (*Camellia sinensis* L. Kuntze). Agronomy 9, 1–15. https://doi.org/10.3390/agronomy9070396.

Picó, Y., Alvarez-Ruiz, R., Alfarhan, A.H., El-Sheikh, M.A., Alshahrani, H.O., Barceló, D., 2020. Pharmaceuticals, pesticides, personal care products and microplastics contamination assessment of Al-Hassa irrigation network (Saudi Arabia) and its shallow lakes. Sci. Total Environ. 701, 135021. https://doi.org/10.1016/j.scitotenv.2019.135021.

Qian, J., Chen, Q., Ward, S.M., Duan, E., Zhang, Y., 2019. Impacts of caffeine during pregnancy. Trends Endocrinol. Metabol. 1–10 https://doi.org/10.1016/j.tem.2019.11.004.

Rajapaksha, A.U., Vithanage, M., Ahmad, M., Seo, D.C., Cho, J.S., Lee, S.E., Lee, S.S., Ok, Y.S., 2015. Enhanced sulfamethazine removal by steam-activated invasive plant-derived biochar. J. Hazard Mater. 290, 43–50. https://doi.org/10.1016/j.jhazmat.2015.02.046.

Richards, S., Withers, P.J.A., Paterson, E., McRoberts, C.W., Stutter, M., 2017. Removal and attenuation of sewage effluent combined tracer signals of phosphorus, caffeine and saccharin in soil. Environ. Pollut. 223, 277–285. https://doi.org/10.1016/j.envpol.2017.01.024.

Roberts, D.A., de Nys, R., 2016. The effects of feedstock pre-treatment and pyrolysis temperature on the production of biochar from the green seaweed Ulva. J. Environ. Manag. 169, 253–260. https://doi.org/10.1016/j.jenvman.2015.12.023.

Roberts, D.A., Paul, N.A., Dworjanyn, S.A., Bird, M.I., De Nys, R., 2015. Biochar from commercially cultivated seaweed for soil amelioration. Sci. Rep. 5, 1–6. https://doi.org/10.1038/srep09665.

Scheufele, F.B., Módenes, A.N., Borba, C.E., Ribeiro, C., Espinoza-Quiñones, F.R., Bergamasco, R., Pereira, N.C., 2016. Monolayer-multilayer adsorption phenomenological model: kinetics, equilibrium and thermodynamics. Chem. Eng. J. 284, 1328–1341. https://doi.org/10.1016/j.cej.2015.09.085.

Senthilkumar, R., Reddy Prasad, D.M., Govindarajan, L., Saravanakumar, K., Naveen Prasad, B.S., 2020. Synthesis of green marine algal-based biochar for remediation of arsenic(V) from contaminated waters in batch and column mode of operation. Int. J. Phytoremediation 22, 279–286. https://doi.org/10.1080/15226514.2019.1658710.

Shenzhen, T., 2015. Emission spectra of Tb^{3+}: Zn_2SiO_4 and Eu^{3+}: Zn_2SiO_4 sol-gel powder phosphors. J. Spectrosc. Dyn. 4 (5), 1–8.

Singh, D.K., Kumar, V., Mohan, S., Bano, D., Hasan, S.H., 2017. Breakthrough curve modeling of graphene oxide aerogel packed fixed bed column for the removal of Cr (VI) from water. J. Water Process Eng. 18, 150–158. https://doi.org/10.1016/j.jwpe.2017.06.011.

Song, G., Guo, Y., Li, G., Zhao, W., Yu, Y., 2019. Comparison for adsorption of tetracycline and cefradine using biochar derived from seaweed *Sargassum sp*. Desalin. Water Treat. 160, 316–324. https://doi.org/10.5004/dwt.2019.24333.

Sonon, L.S., Kissel, D.E., Saha, U., 2017. Cation Exchange Capacity and Base Saturation-UGA Cooperative Extension Circular 1040.

Stromer, B.S., Woodbury, B., Williams, C.F., 2018. Tylosin sorption to diatomaceous earth described by Langmuir isotherm and Freundlich isotherm models. Chemosphere 193, 912–920. https://doi.org/10.1016/j.chemosphere.2017.11.083.

Swami, S., 2017. Test your soil, don't guess: scientific method of ccollecting good soil sample for testing. In: Singh, R., Thakur, N.S.A., Noren, S.K., Singh, R.J., Devarani, L., Kennedy, N. (Eds.), Enhancing Socio-Economic Status and Livelihood Security of Tribal Farmers of Meghalaya, pp. 143–146.

Tasho, R.P., Cho, J.Y., 2016. Veterinary antibiotics in animal waste, its distribution in soil and uptake by plants: a review. Sci. Total Environ. 563–564, 366–376. https://doi.org/10.1016/j.scitotenv.2016.04.140.

Tran, H.N., Wang, Y.F., You, S.J., Chao, H.P., 2017. Insights into the mechanism of cationic dye adsorption on activated charcoal: the importance of Π–Π interactions. Process Saf. Environ. Protect. 107, 168–180. https://doi.org/10.1016/j.psep.2017.02.010.

Vithanage, M., Herath, I., Almaroai, Y.A., Rajapaksha, A.U., Huang, L., Sung, J.K., Lee, S. S., Ok, Y.S., 2017. Effects of carbon nanotube and biochar on bioavailability of Pb, Cu and Sb in multi-metal contaminated soil. Environ. Geochem. Health 39, 1409–1420. https://doi.org/10.1007/s10653-017-9941-6.

Vithanage, M., Rajapaksha, A.U., Tang, X., Thiele-Bruhn, S., Kim, K.H., Lee, S.E., Ok, Y. S., 2014. Sorption and transport of sulfamethazine in agricultural soils amended with invasive-plant-derived biochar. J. Environ. Manag. 141, 95–103. https://doi.org/10.1016/j.jenvman.2014.02.030.

Volkow, N.D., Wang, G.J., Logan, J., Alexoff, D., Fowler, J.S., Thanos, P.K., Wong, C., Casado, V., Ferre, S., Tomasi, D., 2015. Caffeine increases striatal dopamine D2/D3 receptor availability in the human brain. Transl. Psychiatry 5. https://doi.org/10.1038/tp.2015.46 e549-6.

Xing, Z., Tian, K., Du, C., Li, C., Zhou, J., Chen, Z., 2019. Agricultural soil characterization by FTIR spectroscopy at micrometer scales: depth profiling by photoacoustic spectroscopy. Geoderma 335, 94–103. https://doi.org/10.1016/j.geoderma.2018.08.003.

Xu, J., Wu, L., Chang, A.C., 2009. Degradation and adsorption of selected pharmaceuticals and personal care products (PPCPs) in agricultural soils. Chemosphere 77, 1299–1305. https://doi.org/10.1016/j.chemosphere.2009.09.063.

Xu, X., Du, C., Ma, F., Shen, Y., Zhou, J., 2020. Forensic soil analysis using laser-induced breakdown spectroscopy (LIBS) and Fourier transform infrared total attenuated reflectance spectroscopy (FTIR-ATR): principles and case studies. Forensic Sci. Int. 310, 110222. https://doi.org/10.1016/j.forsciint.2020.110222.

Zhang, C., Zhang, L., Gao, J., Zhang, S., Liu, Q., Duan, P., Hu, X., 2020. Evolution of the functional groups/structures of biochar and heteroatoms during the pyrolysis of seaweed. Algal Res 48, 101900. https://doi.org/10.1016/j.algal.2020.101900.

Zhang, D., Gersberg, R.M., Ng, W.J., Tan, S.K., 2014. Removal of pharmaceuticals and personal care products in aquatic plant-based systems: a review. Environ. Pollut. 184, 620–639. https://doi.org/10.1016/j.envpol.2013.09.009.

Zhang, T., Wu, B., Sun, N., Ye, Y., Chen, H., 2013. Sorption and degradation of wastewater-associated pharmaceuticals and personal care products in agricultural soils and sediment. Water Sci. Technol. 68, 991–998. https://doi.org/10.2166/wst.2013.326.

Zhao, B., O'Connor, D., Zhang, J., Peng, T., Shen, Z., Tsang, D.C.W., Hou, D., 2018. Effect of pyrolysis temperature, heating rate, and residence time on rapeseed stem derived biochar. J. Clean. Prod. 174, 977–987. https://doi.org/10.1016/j.jclepro.2017.11.013.